2018

Enabling Highly Effective Boiling from Superhydrophobic Surfaces

T. Allred

J. A. Weibel
Purdue University, jaweibel@purdue.edu

S V. Garimella
Purdue University, sureshg@purdue.edu

Allred, T.; Weibel, J. A.; and Garimella, S V., "Enabling Highly Effective Boiling from Superhydrophobic Surfaces" (2018). *CTRC Research Publications*. Paper 328.
http://dx.doi.org/10.1103/PhysRevLett.120.174501

Enabling Highly Effective Boiling from Superhydrophobic Surfaces

Taylor P. Allred, Justin A. Weibel, and Suresh V. Garimella
School of Mechanical Engineering and Birck Nanotechnology Center, Purdue University, West Lafayette, Indiana 47907, USA

(Received 9 January 2018; published 27 April 2018)

A variety of industrial applications such as power generation, water distillation, and high-density cooling rely on heat transfer processes involving boiling. Enhancements to the boiling process can improve the energy efficiency and performance across multiple industries. Highly wetting textured surfaces have shown promise in boiling applications since capillary wicking increases the maximum heat flux that can be dissipated. Conversely, highly nonwetting textured (superhydrophobic) surfaces have been largely dismissed for these applications as they have been shown to promote formation of an insulating vapor film that greatly diminishes heat transfer efficiency. The current Letter shows that boiling from a superhydrophobic surface in an initial Wenzel state, in which the surface texture is infiltrated with liquid, results in remarkably low surface superheat with nucleate boiling sustained up to a critical heat flux typical of hydrophilic wetting surfaces, and thus upends this conventional wisdom. Two distinct boiling behaviors are demonstrated on both micro- and nanostructured superhydrophobic surfaces based on the initial wetting state. For an initial surface condition in which vapor occupies the interstices of the surface texture (Cassie-Baxter state), premature film boiling occurs, as has been commonly observed in the literature. However, if the surface texture is infiltrated with liquid (Wenzel state) prior to boiling, drastically improved thermal performance is observed; in this wetting state, the three-phase contact line is pinned during vapor bubble growth, which prevents the development of a vapor film over the surface and maintains efficient nucleate boiling behavior.

DOI: 10.1103/PhysRevLett.120.174501

Boiling is central to heat exchange processes in staple industries such as power generation and water distillation and has emerged as the primary choice when extremely high heat fluxes need to be dissipated from high-power electronic systems and nuclear reactors. While boiling has been implemented in practical systems for decades, a lack of understanding of several fundamental aspects and key phenomenological limits has prevented the rational design of enhanced surfaces for use in industry. In particular, a key limiting phenomenon that constrains system operations is the critical heat flux (CHF), a catastrophic point of failure at which the surface is blanketed completely by vapor and the efficiency of heat transport is throttled by orders of magnitude compared to nucleate boiling. Long since the seminal theory for critical heat flux proposed by Zuber [1] purely based on hydrodynamic considerations of the vapor interaction with liquid above the surface, it has been shown that conventional theories cannot explain the significant role of the surface characteristics of wettability and texturing in boiling and CHF [2–7]. Surface modifications must be designed such that the efficiency of nucleate boiling is enhanced (i.e., heat transfer coefficient, representing the rate of heat transport across a given temperature differential, is maximized), while the onset of critical heat flux is delayed.

The wettability of a surface can be most simply defined based on the static contact angle (CA) formed by a sessile droplet; for water, a surface with a CA of less than 90 deg is considered hydrophilic, while one greater than 90 deg is considered hydrophobic. On superhydrophilic surfaces (commonly, textured hydrophilic surfaces), liquid spreads completely and forms a near-zero CA. At the other end of the spectrum, textured hydrophobic surfaces can yield drastically different behavior, depending on which of two distinct wetting states is attained. Superhydrophobic behavior, characterized by static CA exceeding 150 deg with roll-off angle less than 10 deg, is indicative of the Cassie-Baxter state [8] in which the liquid rests on top of surface structures. While engineered surfaces can exhibit an extreme CA exceeding 170 deg and roll-off angle of less than 1 deg [9,10], this behavior is only achieved in a metastable Cassie-Baxter state on the surface [11,12]. An alternative stable equilibrium may be achieved in the Wenzel state, where the liquid fully infiltrates the surface structures. The *static* CA in this state is higher than on a flat hydrophobic surface of the same material [13,14], but droplets become pinned in the surface structures, leading to a drastically different *dynamic* contact angle behavior, namely, increased resistance to three-phase contact line motion compared with the Cassie-Baxter state [15].

Surface wettability has been shown to influence a number of aspects of boiling heat transfer, including the superheat required for incipience, bubble departure characteristics, and critical heat flux [2,4–6,16–19]. In general, heat transfer coefficients during nucleate boiling are higher

TABLE I. Summary of boiling behavior of water from textured superhydrophobic surfaces.

Author(s)	Surface modification	Contact angle	Onset of film boiling
Takata *et al.* [22]	Nickel plated surface with PTFE microparticle coating	150–170 deg	~5–6 °C superheat; ~5 W/cm^2
Hsu and Chen [23]	Silica nanoparticles with fluorosilane coating	149–155 deg	Upon incipience
Malavasi *et al.* [24]	Stainless steel with commercial hydrophobic coating (Glaco Mirror Coat Zero, Soft99 Co)	~150 deg	Upon incipience
Li *et al.* [25]	Silicon nanowires with PTFE coating	>150 deg	Upon incipience
Teodori *et al.* [26]	Stainless steel with commercial nanoparticle coating (Glaco Mirror Coat Zero, Soft99 Co)	~165 deg	Upon incipience at ~1 °C superheat
Current study	Laser-etched copper surface with PDMS coating	158 deg	Initial Cassie-Baxter state: <2 W/cm^2; initial Wenzel state: 115 W/cm^2

for less wetting surfaces, as a result of lowered incipience superheat and higher bubble nucleation density; conversely, critical heat flux is higher for more wetting surfaces, due to effective rewetting of the surface. This trade-off between two desirable performance traits as a function of surface wettability is stark when extreme surface wettability differences are considered. Textured superhydrophilic surfaces have shown significant enhancement of CHF through capillary wicking, albeit with delayed incipience and moderately reduced heat transfer coefficients during boiling; they have been thoroughly investigated for high-heat-flux boiling applications [5,20,21]. Conversely, superhydrophobic surfaces have been observed to drastically reduce the critical heat flux, often immediately transitioning to film boiling at boiling incipience, with little or no nucleate boiling observed, as summarized in Table I [22–26]; despite any potential increase in the heat transfer coefficient, the narrow range of nucleate boiling operation has precluded consideration of superhydrophobic surfaces for practical boiling applications. In an attempt to utilize the favorable boiling characteristics of hydrophobicity, without the concomitant reduction in CHF, heterogeneous surfaces have recently been proposed that add hydrophobic regions to act as nucleation sites on hydrophilic surfaces [27,28]; in some cases, simultaneous improvement in the heat transfer coefficient and CHF has been observed compared to uniform hydrophilic surfaces [29–31].

Because the two possible wetting states on textured superhydrophobic surfaces display drastically different dynamic contact line behavior, which has been proposed to play a critical role in boiling critical heat flux [2], it is reasonable to expect these wetting states to yield different boiling behavior. Because of the increased contact line pinning, it is hypothesized that a superhydrophobic surface with an initial Wenzel state during boiling will limit vapor spreading and maintain nucleate boiling to a much higher critical heat flux than if in the Cassie-Baxter state, which has a low CA hysteresis. In this study, micro- and nanostructured superhydrophobic surfaces are fabricated and evaluated in pool boiling experiments. The initial wetting state is controlled to be either in a Wenzel state or Cassie-Baxter state for each surface tested, and a remarkable increase in the critical heat flux is observed for the Wenzel state compared to early onset of film boiling at a minimal superheat for the Cassie-Baxter state. While previous studies on boiling on superhydrophobic surface in the literature did not specifically note the wetting state encountered, it is expected that all surfaces and test procedures in these past studies (Table I) naturally promoted the less-favorable Cassie-Baxter state.

Two different superhydrophobic surfaces, one microstructured and one nanostructured, were fabricated directly on the surfaces of copper test blocks. The microstructured copper surface was fabricated through laser etching (ULS, PLS6MW) to produce a texture with grooves that are tens of micrometers in dimension, covered with micron-sized fused particles [Fig. 1(a)]. The nanostructured copper surface was fabricated through chemical etching to produce copper oxide nanowires with diameters of $\sim 100 - 300$ nm [Fig. 1(b)]. The surfaces were each coated with polydimethylsiloxane (PDMS) to impart superhydrophobic behavior. The static contact angles, Cassie-state roll-off angles, and Wenzel-state roll-off angles were measured to characterize the wetting behavior (Table II). Further details on the fabrication and characterization procedures are found in the Supplemental Material [32].

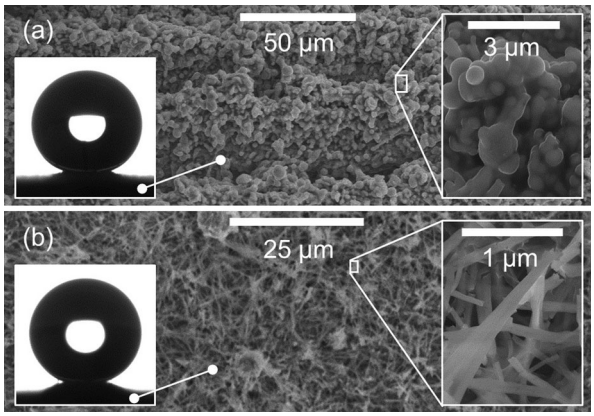

FIG. 1. Scanning electron microscope (SEM) images of (a) the laser-etched microstructured copper surface (300×; top-right inset at 4000×) and (b) the chemically etched nanostructured copper surface (800×; top-right inset at 15 000×). Insets at bottom left of each frame show a static 5 μl droplet resting on the respective surface in the Cassie-Baxter state.

TABLE II. Cassie-Baxter and Wenzel wetting behavior characterization.

Surface	Cassie-Baxter CA	Cassie-Baxter roll-off angle	Wenzel roll-off angle
Microstructured superhydrophobic	158 deg	10 deg	No roll-off
Nanostructured superhydrophobic	165 deg	~1 deg	No roll-off

The superhydrophobic surfaces are sealed into a test chamber for evaluation of boiling performance (detailed information on the experimental facility is provided in the Supplemental Material [32]). The process used for degassing the liquid in the chamber is critical to determining the initial wetting state of the surface and has been shown to impact the incipience behavior of textured hydrophobic surfaces [35]. When liquid is filled into the chamber, an air film remains trapped within the superhydrophobic surface texture. Degassing of the liquid in the chamber requires boiling and recondensing of the vapor while noncondensables are purged from the system. On the one hand, if the liquid is degassed by boiling off the surface (process used to obtain initial Cassie-Baxter state), the vapor produced during boiling replaces the air within the surface texture features; the vapor remains in the interstices throughout the test without recondensing because the pool is maintained at the saturation temperature. If, on the other hand, separate immersion heaters in the pool are used to degas the liquid, without any boiling off the surface, the trapped air diffuses from the surface into the liquid and is eventually removed from the system; degassed liquid floods the surface texture and an initial Wenzel state is achieved. Once the system is degassed and the desired initial wetting state of the surface is achieved, the chamber is sealed and the experiment begins. At a fixed chamber pressure, heat flux is supplied in increments to the surface and the system is allowed to reach steady-state operation at each heat flux; high-speed flow visualizations are recorded at steady state, along with the readings of surface superheat. Reported error bars are determined based on the measurement uncertainties within the system. Details of the experimental procedure and data analysis are provided in the Supplemental Material [32].

For both the microstructured and the nanostructured surfaces, a contrast in the boiling behavior was observed between an initial Cassie-Baxter state and an initial Wenzel state. The behavior is demonstrated in Fig. 2 for the nanostructured surface, which exhibits the more extreme nonwetting nature. When the experiment started with the surface in the Cassie-Baxter state, film boiling occurred shortly after incipience, prior to reaching steady-state conditions for the first heat flux test point of 2.1 W/cm^2, matching the behavior commonly observed for superhydrophobic surfaces in the literature; film boiling continued as the heat flux was increased [see Fig. 2(d)]. In contrast, for an initial Wenzel wetting state, a nucleate boiling mode consisting of individual bubbles nucleating and departing from the surface at a high density was observed [see Fig. 2(h)]. This hitherto unreported nucleate boiling behavior on a nanostructured superhydrophobic surface continued up to a heat flux of 45 W/cm^2, at which point testing ceased. The boiling data for this surface are presented in the Supplemental Material [32]. Critical heat flux was avoided in order to prevent damage to the surface associated with the

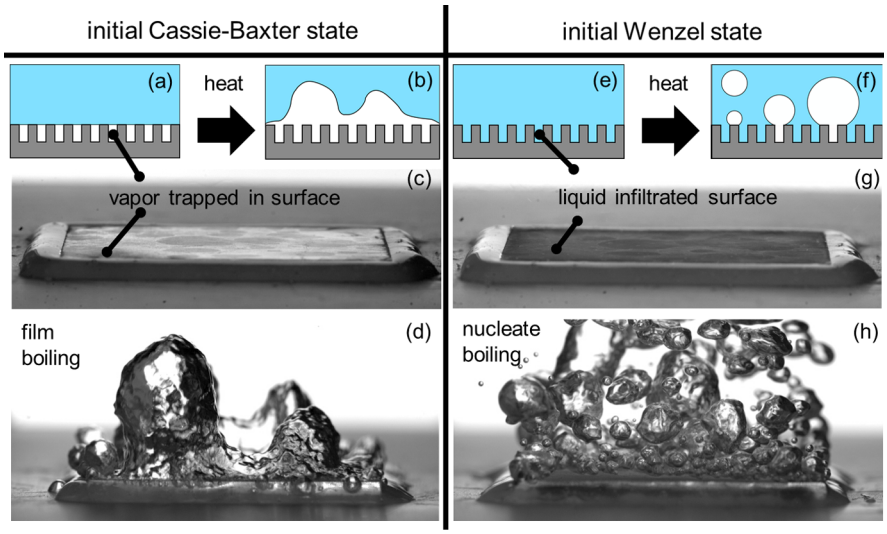

FIG. 2. Illustrations of (a) the initial Cassie-Baxter state progressing to (b) film boiling upon heating and (e) the initial Wenzel state progressing to (f) nucleate boiling upon heating. Visualization of (c) the initial Cassie-Baxter state and (d) subsequent film boiling from a submerged nanostructured superhydrophobic surface (heat flux 9 W/cm^2, surface superheat 17.7 °C). Visualization of (g) the initial Wenzel state and (h) subsequent nucleate boiling from a submerged nanostructured superhydrophobic surface (7.6 W/cm^2, 7.4 °C). High-speed visualizations of each case, over a range of heat fluxes, are available in Video S1 of the Supplemental Material [32].

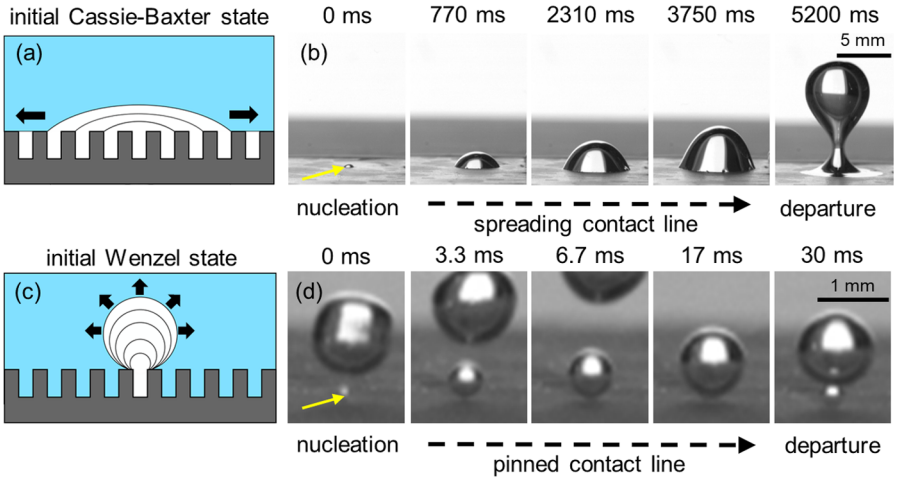

FIG. 3. Illustrations showing the bubble growth and departure behavior from an (a) initial Cassie-Baxter state and (c) initial Wenzel state and (b),(d) respective image sequences of these behaviors on a nanostructured superhydrophobic surface just after incipience (note the different length and timescales indicated). High-speed visualizations are available in Video S3 of the Supplemental Material [32].

sharp temperature excursion, in order to allow confirmation that the observed nucleate boiling behavior was not a result of a loss of superhydrophobicity; a video confirming the posttest superhydrophobicity of the surface is presented as Video S2 in the Supplemental Material [32].

The contrast in boiling behavior between the two initial wetting states is explained by differences in the resistance to three-phase contact line motion in the two states. The contact line moves freely in the Cassie-Baxter state, as demonstrated by the small droplet roll-off angles (see Table II). During boiling, this free movement of the contact line is sustained; the contact diameter of each bubble is free to grow until the bubble becomes large enough (several millimeters in size) to experience necking, pinch-off, and departure, leaving behind a vapor patch on the surface [Fig. 3(b)]. As a result, a single active nucleation site covers a significant amount of surface area with vapor; a small number of nucleation sites can thus coalesce to coat the entire surface in vapor, resulting in film boiling at a minimal heat flux. Conversely, the three-phase contact line is strongly pinned in the Wenzel state, as evidenced by the adherence of a droplet to the surface even when inverted (Table II). As the bubble grows, the contact diameter remains fixed, covering a small region on the surface, and the bubble maintains a spherical shape as a result of the contact line pinning [Fig. 3(d)]. This observation is in contrast to all prior reports of bubble growth on nominally superhydrophobic surfaces in the literature (Table I). These results reveal that the static contact angle of a droplet, which would be large in both Cassie-Baxter and Wenzel states, is not representative of the bubble characteristics following nucleation on textured superhydrophobic surfaces during boiling. Rather, the boiling behavior is governed by contact line dynamics, which are in turn driven by the initial wetting state of the surface.

This demonstration of the ability to maintain nucleate boiling on superhydrophobic surfaces changes our perspective on their potential use as enhanced surfaces. To illustrate that this behavior is not unique to the nanostructured surface shown, the boiling performance is investigated for a microstructured surface in the Cassie-Baxter and Wenzel initial states. For reference, a bare microstructured copper surface without the PDMS coating is also included in the comparison. Boiling curves for the three cases are shown in Fig. 4(a). The reference microstructured bare copper surface has relatively few active nucleation sites at low heat fluxes (<50 W/cm^2), leading to a significant temperature increase with increasing heat

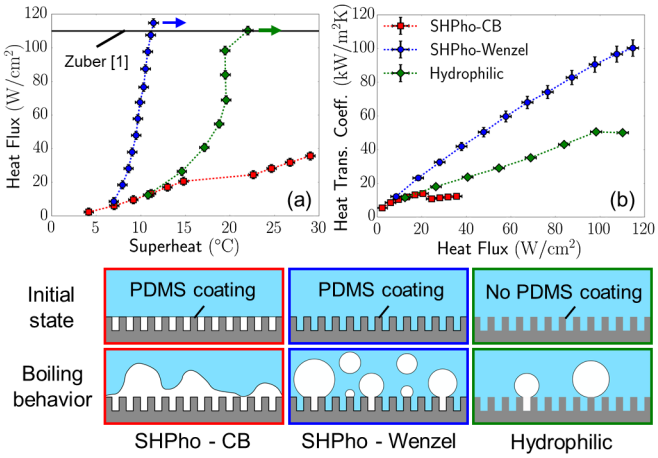

FIG. 4. (a) Boiling curves (surface heat flux as a function of superheat) and the associated (b) heat transfer coefficients for the three microstructured surface cases: superhydrophobic in the Cassie-Baxter state (SHPho-CB), superhydrophobic in the Wenzel state (SHPho-Wenzel), and bare copper (Hydrophilic). Illustrations below the graphs indicate the relationship between the initial wetting state and the boiling behavior. High-speed visualizations are provided in Video S4 of the Supplemental Material [32].

flux. Above 50 W/cm^2, active nucleation over a majority of the surface leads to a sharp increase in the slope of the boiling curve. Nucleate boiling is observed until CHF occurs at 110 W/cm^2, matching the limit predicted by Zuber [1]. The nucleate boiling behavior observed is not a fleeting condition; nucleate boiling on the surface was observed for durations of over 5 h during acquisition of the data. For the case with the initial Cassie-Baxter wetting state, film boiling occurs for all heat fluxes along the boiling curve, with no nucleate boiling regime being observed. Much higher levels of superheat result as compared to the reference bare copper surface, the disparity increasing as the heat flux is increased. The surface in the initial Wenzel wetting state displays nucleate boiling behavior over the entire range of heat fluxes, displaying a minimal rise in surface temperature with increasing heat flux all the way to the critical heat flux. A 100% increase in the maximum heat transfer coefficient [calculated as the heat flux divided by the surface superheat and as shown in Fig. 4(b)] is achieved compared to the bare copper reference; importantly, no reduction in CHF is observed. The substantial increase in heat transfer coefficient is a result of the lower energy requirement for nucleation on hydrophobic substrates [16] leading to a higher nucleation site density. Because of the pinned contact lines of bubbles on the surface in the Wenzel state, bubbles are observed to grow and depart readily, rather than permanently blanketing regions in vapor and diminishing heat transfer, as has been observed for boiling from superhydrophobic surfaces in past studies [30].

This is the first report of sustained, efficient nucleate boiling on a superhydrophobic surface. An initial Wenzel wetting state allows this microstructured superhydrophobic surface to operate in the nucleate boiling regime up to a CHF of 115 W/cm^2, a value comparable to that typical of hydrophilic wetting surfaces; the transition to film boiling occurs at a heat flux over an order of magnitude higher than previous reports for superhydrophobic surfaces [22]. By removing the limiting characteristic of superhydrophobic surfaces of reaching CHF prematurely, their advantageous ability to promote a high nucleation site density can be fully utilized in practical applications that call for high heat transfer coefficients. Heterogeneous surface concepts can utilize superhydrophobic regions primed to operate in the Wenzel state without concern for hot spots or significant deterioration of CHF. It is likely that this Wenzel-state behavior would naturally occur in many industrial applications where surfaces are submerged in water over long periods of time, due to the natural diffusion of air trapped in the surface into the degassed liquid, as has been observed in drag reduction studies [36].

In summary, superhydrophobic surfaces are shown to yield two distinct boiling behaviors based on the wetting state of the surface prior to boiling. Boiling initiated from the Cassie-Baxter state leads to film boiling immediately after incipience, as has been observed in prior studies. For the first time, nucleate boiling is achieved here on a superhydrophobic surface by initiating boiling from a superhydrophobic surface initially brought into the Wenzel state. The strong contact line pinning in the Wenzel state limits contact line spreading, allowing individual bubbles to grow and depart without coalescing into a vapor film. The behavior is demonstrated on two superhydrophobic surfaces of vastly different texture scales—micro- and nanostructured—and is shown to be governed by the initial wetting state of the surface rather than a unique surface structure. Boiling is extremely efficient on superhydrophobic surfaces operating in this mode, owing to their promotion of high nucleation site densities; a nucleate boiling mode is maintained on a superhydrophobic surface up to an unprecedented critical heat flux on the order of the classical Zuber limit [1].

This work was supported as part of Purdue's NEPTUNE Center for Power and Energy, funded by the Office of Naval Research under Grant No. N000141613109. T. P. A. acknowledges support from the Department of Defense (DoD) National Defense Science and Engineering Graduate Fellowship (NDSEG) program, sponsored by the Air Force Office of Scientific Research (AFOSR). We thank Helen Lai and Nicholas Stovall-Kurtz for aiding with operation of the experimental pool boiling facility and Srivathsan Sudhukar for acquiring the SEM images.

[1] N. Zuber, Ph.D. thesis, University of California, Los Angeles, 1959.
[2] S. G. Kandlikar, J. Heat Transfer **123**, 1071 (2001).
[3] B. J. Jones, J. P. McHale, and S. V. Garimella, J. Heat Transfer **131**, 121009 (2009).
[4] H. Jo, H. S. Ahn, S. Kang, and M. H. Kim, Int. J. Heat Mass Transfer **54**, 5643 (2011).
[5] M. M. Rahman, E. Ölçeroğlu, and M. McCarthy, Langmuir **30**, 11225 (2014).
[6] N. S. Dhillon, J. Buongiorno, and K. K. Varanasi, Nat. Commun. **6**, 8247 (2015).
[7] D. E. Kim, D. I. Yu, D. W. Jerng, M. H. Kim, and H. S. Ahn, Exp. Therm. Fluid. Sci. **66**, 173 (2015).
[8] A. B. D. Cassie and S. Baxter, Trans. Faraday Soc. **40**, 546 (1944).
[9] Y. Y. Yan, N. Gao, and W. Barthlott, Adv. Colloid Interface Sci. **169**, 80 (2011).
[10] S. Dash, M. T. Alt, and S. V. Garimella, Langmuir **28**, 9606 (2012).
[11] N. A. Patankar, Langmuir **20**, 7097 (2004).
[12] J. Bico, U. Thiele, and D. Quéré, Colloids Surf., A **206**, 41 (2002).
[13] R. N. Wenzel, Ind. Eng. Chem. **28**, 988 (1936).
[14] R. N. Wenzel, J. Phys. Colloid Chem. **53**, 1466 (1949).
[15] A. Lafuma and D. Quéré, Nat. Mater. **2**, 457 (2003).
[16] H. T. Phan, N. Caney, P. Marty, S. Colasson, and J. Gavillet, Int. J. Heat Mass Transfer **52**, 5459 (2009).

[17] Y. Nam, E. Aktinol, V. K. Dhir, and Y. S. Ju, Int. J. Heat Mass Transfer **54**, 1572 (2011).
[18] A. R. Betz, J. Jenkins, C.-J. Kim, and D. Attinger, Int. J. Heat Mass Transfer **57**, 733 (2013).
[19] Y. Nam and Y. S. Ju, J. Adhes. Sci. Technol. **27**, 2163 (2013).
[20] Y. Takata, S. Hidaka, M. Masuda, and T. Ito, Int. J. Energy Res. **27**, 111 (2003).
[21] B. S. Kim, H. Lee, S. Shin, G. Choi, and H. H. Cho, Appl. Phys. Lett. **105**, 191601 (2014).
[22] Y. Takata, S. Hidaka, and T. Uraguchi, Heat transfer engineering **27**, 25 (2006).
[23] C.-C. Hsu and P.-H. Chen, Int. J. Heat Mass Transfer **55**, 3713 (2012).
[24] I. Malavasi, B. Bourdon, P. Di Marco, J. de Coninck, and M. Marengo, Int. Commun. Heat Mass Transf. **63**, 1 (2015).
[25] Y. Li, K. Zhang, M.-C. Lu, and C. Duan, Int. J. Heat Mass Transfer **99**, 521 (2016).
[26] E. Teodori, T. Valente, I. Malavasi, A. S. Moita, M. Marengo, and A. L. N. Moreira, Appl. Therm. Eng. **115**, 1424 (2017).
[27] X. Wang, Y. Song, and H. Wang, Heat Transfer Res. **44**, 59 (2013).
[28] M. M. Rahman and M. McCarthy, Heat Transfer Eng. **38**, 1285 (2017).
[29] A. R. Betz, J. Xu, H. Qiu, and D. Attinger, Appl. Phys. Lett. **97**, 141909 (2010).
[30] H. Jo, S. Kim, H. S. Park, and M. H. Kim, Int. J. Multiphase Flow **62**, 101 (2014).
[31] M. Zupančič, M. Steinbücher, P. Gregorčič, and I. Golobič, Appl. Therm. Eng. **91**, 288 (2015).
[32] See Supplemental Material at http://link.aps.org/supplemental/10.1103/PhysRevLett.120.174501 for surface fabrication and characterization procedure, experimental details, uncertainty analysis, nanostructured superhydrophobic surface data, and high-speed videos of boiling behavior, which includes Refs. [33,34].
[33] G. W. Burns, M. G. Scroger, G. F. Strouse, M. C. Croarkin, and W. F. Guthrie, Temperature-electromotive force reference functions and tables for the letter-designated thermocouple types based on the ITS-90, https://archive.org/details/temperatureelect175burn.
[34] K. Brown, H. Coleman, and W. Steele, in *Proceedings of the 33rd Aerospace Science Meeting Exhibit* (American Institute of Aeronautics and Astronautics, Washington, D.C., 1995).
[35] B. Shen, M. Yamada, S. Hidaka, J. Liu, J. Shiomi, G. Amberg, M. Do-Quang, M. Kohno, K. Takahashi, and Y. Takata, Sci. Rep. **7**, 2036 (2017).
[36] R. N. Govardhan, G. S. Srinivas, A. Asthana, and M. S. Bobji, Phys. Fluids **21**, 052001 (2009).